randomly stacked intercrystallite or in the tubular spaces of ANS, as revealed in Fig. 1

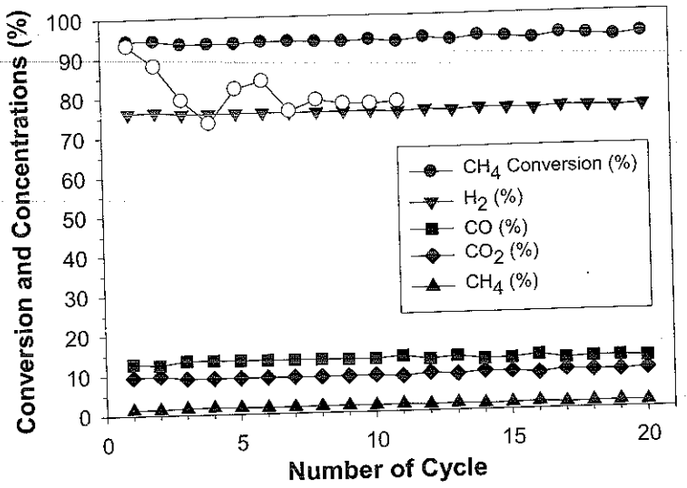

Fig. 2. Thermal cyclic test of supported Ru catalysts for CH_4 steam reforming. Filled symbols (Ru/ANS), unfilled symbol (Ru//γ-Al_2O_3), Thermal cyclic test conditions: Temperature = 700 (°C), S/C=3, GHSV=8000 (h^{-1}).

In conclusion, nanostructured crystalline γ-alumina is an excellent catalytic support which has high surface area and pore volume, high thermal and chemical stability, and unique morphological properties. As shown, these unique properties led to an enhanced activity and stability of Ru/ANS in the steam reforming of methane.

References

1. C. Song, *Catal. Today*, **2002**, *77*, 17.
2. J. R. Rostrup-Nielsen and K. Aasberg-Petersen, in: W. Vielstich, A. Lamm, H.A. Gasteiger(Eds.), Handbook of Fuel Cells: Fundamentals Technology and Application, Part 2, vol. 3, John Wiley & Sons Ltd., West Sussex, **2003**, p.159-176.
3. S. Cabrera, J. E. Haskouri, J. Alamo, A. Beltrán, D. Beltrán, S. Mendioroz, M. D. Marcos and P. Amorós, *Adv. Mater.* **1999**, *11*, 379.
4. S. A. Bagshaw and T. J. Pinnavaia, *Angew. Chem. Int. Ed. Engl.* **1996**, *35*, 1102.
5. H. C. Lee, H. J. Kim, S. H. Chung, K. H. Lee, H. C. Lee and J. S. Lee, *J. Am. Chem. Soc.*, **2003**, *125*, 2882.

Natural Gas Conversion VIII
F.B. Noronha, M. Schmal, E.F. Sousa-Aguiar (Editors)

HEAT EFFECTS IN A MEMBRANE REACTOR FOR THE WATER GAS SHIFT REACTION

M. E. Adrover, E. López, D. O. Borio, M. N. Pedernera

Department of Chemical Engineering - PLAPIQUI
Universidad Nacional del Sur - CONICET
Camino La Carrindanga, Km 7
(8000) Bahía Blanca, ARGENTINA

1. Introduction

Most of the hydrogen is produced industrially by steam reforming of hydrocarbons or alcohols (e.g., for fuel cell applications). The process gas stream coming from the steam reformer is composed by H_2, CO, CO_2, H_2O and small amounts of unconverted reactants (CH_4). The CO concentration of the gas leaving the reformer must be reduced up to a specified level, with two main goals: 1) increase the H_2 production rate and 2) purify the process stream. To these ends, the Water Gas Shift Reaction (WGSR) is widely used:

$$CO + H_2O \Leftrightarrow CO_2 + H_2 \qquad \Delta H^{\circ}_{298K} = -41.09\ kJ/mol \qquad (1)$$

Reaction (1) is moderately exothermic and strongly controlled by the chemical equilibrium, which is favoured at low temperatures. In small-scale processes, such as the fuel processing for fuel cells (e.g., PEM cells) normally the WGSR is carried out in a single reactor at an intermediate temperature level [1].

An attractive alternative to increase the CO conversion is the membrane reactor (MR) (Figure 1). The main idea of this design is the selective permeation of reaction products (e.g., H_2) to

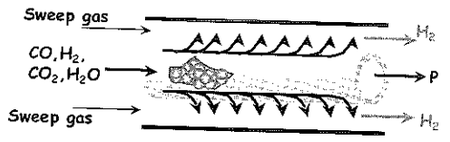

Figure 1: Scheme of the membrane reactor

shift the equilibrium towards products and consequently increase the conversion, or reduce the amount of catalyst for a desired conversion level. For this reason, MRs have deserved considerable attention in the scientific literature [2].

The H_2 removal can be carried out by means of selective dense membranes of Pd or its alloys. In order to decrease the cost and increase the permeation fluxes, composite membranes became an alternative. In these membranes a substrate of high porosity and low resistance to flow is covered by a metallic layer, which provides the selectivity [3-5].

The advantages of the MR to perform the WGSR have been demonstrated by Criscuoli et al. [6]. However, the heat effects were neglected and the reactor operation was supposed to be isothermal. This is a common assumption in the modeling of most of the MRs, which agrees with the temperature measurements inside the reactor at laboratory scale due to the high ratio between the heat transfer area and the reactor volume. This condition may not be true when higher process scales are necessary; e.g.: several membrane tubes installed in parallel within a shell where the sweep gas is circulated. Here, the usual assumption of isothermal MR should be removed and the heat effects taken into account [7-9].

In the present work the performance of the MR for the WGSR is simulated and compared with that of a fixed-bed reactor (CR), for isothermal and adiabatic operations. The analysis is further extended to a MR under non-isothermal non-adiabatic conditions.

2. Mathematical model

The simulation study is carried out by means of a 1-D pseudo-homogeneous mathematical model. The model is subject to the following hypotheses: a) axial and radial mass and heat transfer dispersions are neglected; b) isobaric conditions; c) infinite selectivity for the membrane (H_2 is the permeation gas); d) the permeation flow through the membrane follows Sievert´s law; and e) the shell is adiabatic. The kinetic model proposed for the WGSR by Podolski and Kim [10] is included. The model is represented by the following equations:

Reaction Side (catalyst tubes)

Mass Balances

$$\frac{dF_{CO}}{dz} = A_T r_{CO} \rho_B \quad (2)$$

$$\frac{dF_{H_2}}{dz} = A_T (-r_{CO}) \rho_B - \pi d_{te} J_{H_2} \quad (3)$$

Permeation Side (shell)

Mass Balances

$$\frac{dF_{H_2,P}}{dz} = \pi d_{te} n_t J_{H_2} \quad (4)$$

$$\frac{dF_{SG,P}}{dz} = 0 \quad (5)$$

Energy Balance

$$\frac{dT}{dz} = \frac{A_T \rho_B (-r_{CO})(-\Delta H_r) - \pi d_{te} U (T - T_P)}{\sum_{j=1}^{N} F_j C_{pj}} \quad (6)$$

Energy Balance

$$\frac{dT_P}{dz} = \frac{\pi d_{te} n_t (T - T_P)\left[J_{H_2} C_{pH_2} + U\right]}{\sum_{j=1}^{2} F_{j,P} C_{pj}} \quad (7)$$

where: $J_{H_2} = \frac{7.70\,10^{-5} e^{(-1960.5/T)}}{\delta}\left[\sqrt{p_{H_2}} - \sqrt{p_{H_2,P}}\right]$ (Barbieri et al. [11]) (8)

Boundary conditions

Cocurrent Scheme:

$$\text{At z=0} \begin{cases} F_j = F_{j0} \quad for\ j = 1, 2...., N \\ T = T_0; T_P = T_{P,inlet} \\ F_{H_2,P} = 0; F_{SG,P} = F_{SG,inlet} \end{cases}$$

Countercurrent Scheme:

$$\text{At z=0} \begin{cases} F_j = F_{j0} \quad for\ j = 1,2...., N \\ T = T_0 \end{cases}$$

$$\text{At z=L} \begin{cases} F_{H_2,P} = 0; F_{SG,P} = F_{SG,inlet} \\ T_P = T_{P,inlet} \end{cases}$$

The design parameters and operating conditions are given in Table 1. The CR is modeled by assuming zero for the hydrogen flow through the membrane. For both reactors, two different configurations for the gas through the shell are studied: co- and countercurrent flow.

Table 1. Geometric parameters and operating conditions used in the simulations of CR and MR (Criscuoli et al. [6]*; Giunta et al. [1]**).

L	0.21 m (CR)- 0.15 m (MR) *	U	10 W/(m^2 K)
d_{ti}	6.7 mm (CR)- 8 mm (MR) *	F_0	9.58 10^{-3} mol/s
d_{te}	13.4 mm (MR) *	Inlet CO, %	7.97 **
n_t	30	Inlet CO_2, %	10.99 **
W	9.64 g *	Inlet H_2, %	43.48 **
δ	75 μm*	Inlet H_2O, %	31.88 **
P_o	1 atm *	Inlet CH_4, %	5.68 **
$F_{SG,inlet}$	30 l/min		

3. Results and Discussion

The performance of both reactor designs is first compared for two limit situations regarding heat effects: isothermal and adiabatic operations. For the isothermal case the heat effects are neglected for both the reaction and permeation sides; whereas, for the adiabatic operation the convective heat transfer through the membrane is neglected (U=0), i.e., the only source of heat exchange between both sides is the permeating hydrogen flow.

Figure 2 shows the axial conversion profiles in the MR and CR, at a given inlet temperature, T_{o1}=360 °C. For both CR and MR, the outlet CO conversion corresponding to the adiabatic operation is lower than that of the isothermal case. These results can be attributed to equilibrium limitations. For high inlet temperatures, the assumption of isothermal operation is not conservative and the

CO outlet conversions are overestimated in both types of reactors. Conversely, for low feed temperatures, the adiabatic operation introduces conversion improvements with respect to the isothermal case, for both reactor designs, due mainly to kinetic reasons (results not shown).

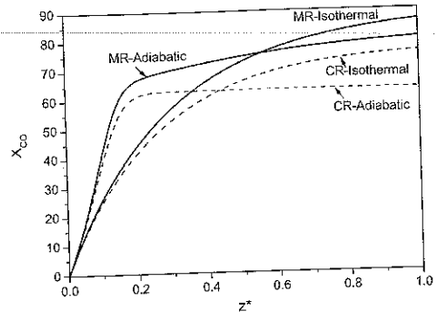

Figure 2: Axial CO conversion in MR and CR. T_{o2}=360°C. Isothermal and adiabatic conditions

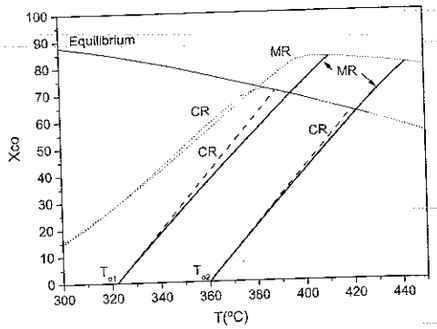

Figure 3: Conversion-temperature trajectories in MR and CR, for T_{o1}=322°C and T_{o2}=360°C.

The adiabatic operation (U=0) in the MR and the CR can also be compared in the phase-plane. Thus, Figure 3 shows the conversion-temperature trajectories inside the adiabatic reactors, for two inlet temperatures. The dotted lines join all the outlet conversion points, obtained by simulation of MR and CR at different inlet temperatures. It is clear that the total temperature rise inside the reactor is higher for the MR, for two main reasons: 1) the CO conversions are higher, i.e., larger amounts of heat are released; 2) the total gas flowrate in the reaction side diminishes along the axial position as a consequence of the H_2 permeation. Therefore, the adiabatic trajectories corresponding to the MR shift away from the classical straight trajectories corresponding to the CR (dashed lines). That is, even for the same conversion level, the temperature rise will be higher in the adiabatic MR than in the adiabatic CR.

The membrane reactor analysis is extended to non-adiabatic conditions for two different flow configurations of the gas flowing through the shell: co- and counter-current. The already reported values for the sweep gas flowrate and the overall heat-transfer coefficient (see Table 1) were kept constant for all the simulations. Figure 4 presents the axial temperature evolutions in the MR for both flow configurations. For co-current operation, the driving force for heat transfer (T-T_P) is high enough at the reactor entrance to maintain the temperature rise in the reaction side below 40 degrees. For the second half of the reactor both temperatures tends to be the same and low convective heat transfer rates are observed. Regarding the counter-current scheme, as the sweep gas temperature is higher than the reaction temperature near the entrance, the sweep gas acts as a heating medium. Consequently, the reaction temperature

rises up to much higher values than in the co-current case (around 70°C). This phenomenon may cause a faster catalyst deactivation. Near the reactor outlet the cooling effect of the sweep gas causes an increase in the reaction rates.

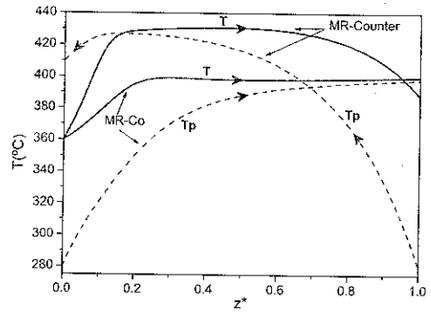

Figure 4: Axial temperature profiles of reaction (T) and permeation (T_P) sides in MR. T_o=360°C, $T_{P,inlet}$=280°C, $F_{SG,inlet}$ and U as reported in Table 1. Non-adiabatic conditions.

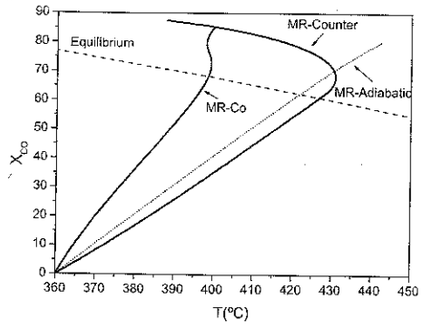

Figure 5: Conversion vs. Temperature trajectories in MR, for adiabatic and non-adiabatic operations (co- and counter-current schemes). Same conditions as in Figure 4.

Results in the phase-plane are presented in Figure 5. The CO outlet conversions under non-adiabatic conditions are around 85-90%, which determine CO levels in the order of 1-2% (dry basis), suitable to be fed to a PrOx reactor. When co-current configuration is analysed, a slight hot spot is observed. Besides, the increment in the CO conversion due to the permeation effects (shifting of the equilibrium) is the source of a slight temperature minimum (or cold spot). On the other hand, the hot spot detected in counter-current operation is considerable and the total temperature rise inside the reactor is similar to the adiabatic case. Under this flow configuration, the observed parametric sensitivity with respect to the sweep gas inlet temperature ($T_{P,inlet}$) was extremely high. This result may be a consequence of the selected sweep gas flowrate; higher sweep gas flowrates lead to lower sensitivities and flatter counter-current temperature profiles. However, higher power requirements are necessary and permeate streams with lower H_2 concentrations are obtained. For the studied operating condition, the co-current scheme appears as the most convenient configuration, as the desirable conversion level can be obtained with a temperature rise of about half of the other operations under analysis.

4. Conclusions

For adiabatic operation, the total temperature rise inside the reactor is higher for the MR due to the higher CO conversions achieved and the diminution of the total gas flowrate in the reaction side, as a consequence of the H_2 permeation. When non-adiabatic conditions are considered, the proper selection

of the operating conditions for the shell side becomes a key factor to avoid undesirable temperature raises over the catalyst and high parametric sensitivity.

The previous results point out over the need to consider the heat effects in membrane reactors. Although the WGSR is moderately exothermic, the temperature changes inside the reactor are not negligible. The only reason to neglect the heat effects in MRs is the small scale of laboratory designs. When intermediate (or large) scales are under consideration, the temperature variations will affect the kinetics and the chemical equilibrium.

Regarding the selected application, the simulated non-adiabatic membrane reactors show an adequate performance in terms of reaching CO outlet concentrations of between 1 and 2%, suitable values to directly feed a final purification unit for fuel-cell applications.

5. Nomenclature

A_T = cross sectional area of tubes, m^2
C_{pj} = specific heat of component j, kJ/(mol K)
d_{te} = external tube diameter, m
F_j = molar flow of component j, mol/s
J_{H2} = permeation flow of hydrogen, mol/(s m^2)
L = tube length, m
N = number of components (reaction side)
n_t = number of tubes
p_{H2} = partial pressure of hydrogen, Pa
r_{CO} = reaction rate , mol_{CO}/(kg_{cat} s)
T = temperature, K
U = overall heat transfer coefficient, kJ/(s m^2 K)
W = catalyst mass, g
z = axial coordinate, m
δ = thickness of Pd film, m
ΔH_r = heat of reaction, kJ/mol
ρ_B = bed density, kg_{cat}/m^3

Subscripts
CO = carbon monoxide
H_2 = hydrogen
j = component j
L = at the axial coordinate $z=L$
P = at permeation side
SG = sweep gas
0 = at the axial coordinate $z=0$

6. References

[1] P. Giunta, N. Amadeo, M. Laborde, XIV Cong. Arg. Catal., Arg., (2005) 610.
[2] J. Coronas, J. Santamaría, Catal. Today, 51 (1999) 377.
[3] J. S. Oklany, K. Hou, R. Hughes, App. Catal. A, 170 (1998) 13.
[4] S. Tosti L. Bettinali, V. Violante, Int. J. Hyd. Energy, 25 (2000) 319.
[5] W.H. Lin, H.F. Chang, Surf. Coat. Tech., 194 (2005) 157.
[6] Criscuoli, A. Basile, E. Drioli, Catal. Today, 56 (2000) 53.
[7] M. Bratch, P. Alderliesten, R. Kloster, R. Pruschek, G. Haupt, E. Xue, J. Ross, M. Koukou, N. Papayannakos, En. Conv. Manag., 38 (1997) 159.
[8] M. Koukou, G. Chaloulou, N. Papayannakos, N. Markatos, Int. J. Heat and Mass Tranf., 40 (1997) 2407.
[9] N. Itoh, T. Wu, J. Memb. Sci., 124 (1997) 213.
[10] W. F. Podolski Y. G. ,Kim, Ind. Eng. Chem.,13(4) (1974) 415.
[12] G. Barbieri, A. Brunetti, T. Granato, P. Bernardo, E. Drioli, Ind. Eng. Chem. Res.,

Natural Gas Conversion VIII
F.B. Noronha, M. Schmal, E.F. Sousa-Aguiar (Editors)

Au/ZnO and the PROX REACTION.

Kátia R. Souza, Adriana F.F. de Lima, Fernanda F. de Sousa and Lucia Gorenstin Appel*

Instituto Nacional de Tecnologia / MCT, Av. Venezuela 82 / sala 518,CEP 20081-312, Rio de Janeiro, Brazil Fax: 55 21-21231165 E-mail: appel@uol.com.br

1. Introduction

Recently, there has been a growing interest in gold catalysts due to their potential use in many important reactions that can be employed in industrial and environmental processes. The most important application of these systems is the CO oxidation.
This occurs because preferential CO oxidation (PROX) is the cheapest way to reduce CO concentration in an H_2 stream used as a fuel cell feedstock (PEM).
Many gold catalysts have been studied for CO oxidation and some authors have suggested a very important role for the supports (1). In fact, Au/TiO_2 and Au/Fe_2O_3 are considered to be very active systems (2,3). However, it is well known that they are not stable in the presence of H_2O and CO_2.
According to some authors, Au/ZnO (4) shows good activity and stability for CO oxidation. Nevertheless, there is very little information available in relation to this catalyst in the literature (4-7). In a previous work, we discussed the synthesis of these systems. The results showed that anionic exchange provides small gold particles and also that synthesis conditions modify the gold concentration in the catalysts (8).
The present work aims at contributing to further investigation of gold based zinc oxide catalyst on the preferential CO oxidation (PROX).